Electronic Supplementary Information

Cycloplatinated(II) complexes bearing O,S-heterocyclic ligand: searching for anticancer drugs

Masood Fereidoonnezhad,[a] *Zahra Ramezani,*[a] *Mahshid Nikravesh,*[b] *Jalalaldin Zangeneh,*[a] *Mohsen Golbon Haghighi,*[c] *Zahra Faghih,*[d] *Behrouz Notash,*[c] *and Hamid R. Shahsavari*[b]*

[a]Cancer, Environmental and Petroleum Pollutants Research Center; Department of Medicinal Chemistry, School of Pharmacy, Ahvaz Jundishapur University of Medical Sciences, Ahvaz, Iran.

[b]Department of Chemistry, Institute for Advanced Studies in Basic Sciences (IASBS), Zanjan 45137-66731, Iran.

[c]Department of Chemistry, Shahid Beheshti University, Evin, Tehran 19839-69411, Iran.

[d]Shiraz Institute for Cancer Research, School of Medicine, Shiraz University of Medical Sciences, Shiraz, Iran.

Email: shahsavari@iasbs.ac.ir

Contents:	**Page**
Figure S1. ^{1}H NMR (down) and HH COSY (up) spectra of **2a** in CD_2Cl_2 at room temperature. The signals assignments are depicted and the platinum satellites are indicated by *.	3
Figure S2. $^{13}C\{^{1}H\}$ NMR spectrum of **2a** in CD_2Cl_2.	4
Figure S3. DEPT 135° spectrum of **2a** in CD_2Cl_2.	5
Figure S4. $^{195}Pt\{^{1}H\}$ NMR spectrum of **2a** in CD_2Cl_2.	6
Figure S5. ^{1}H NMR spectrum of **2b** in CD_2Cl_2.	7
Figure S6. $^{13}C\{^{1}H\}$ NMR spectrum of **2b** in CD_2Cl_2.	8
Figure S7. DEPT 135° spectrum of **2b** in CD_2Cl_2.	9
Figure S8. $^{195}Pt\{^{1}H\}$ NMR spectrum of **2b** in CD_2Cl_2.	10
Figure S9. The calculated possible structures for SpyO ligand while it coordinated to **1**.	11
Table S1. Crystallographic and structure refinement data for **2a**.	12
Figure S10. The crystal packing of **2a**.	13
Figure S11. Complex **2a** is displaying the intermolecular contacts. The supramolecular packing is formed by dimers supported by intermolecular π···π interactions involving two SpyO ligands.	13
Table S2. Fragment contributions (%; from atomic orbital contributions) to the frontier orbitals of **2a** in CH_2Cl_2 solution.	14
Table S3. Fragment contributions (%; from atomic orbital contributions) to the frontier orbitals of **2b** in CH_2Cl_2 solution.	14
Table S4. Selected vertical singlet excitations of **2a** from TD-DFT calculations at the ground state geometry in CH_2Cl_2 solution (M = Pt, L = ppy, L' = SpyO).	15
Table S5. Selected vertical singlet excitations of **2b** from TD-DFT calculations at the ground state geometry in CH_2Cl_2 solution (M = Pt, L = bzq, L' = SpyO).	15
Figure S12. MO plots for **2a.**	16
Figure S13. MO plots for **2b.**	16
Figure S14. 3D ligand-receptor interactions of **2a** with DNA (PDB code: 1BNA).	17
Figure S15. 3D ligand-receptor interactions of **2b** with DNA (PDB code: 1BNA).	18
Figure S16. 3D ligand-receptor interactions of **2a** with DNA (PDB code: 198D).	19
Figure S17. 3D ligand-receptor interactions of **2b** with DNA (PDB code: 198D).	20
Figure S18. 3D ligand-receptor interactions of **2a** with DNA (PDB code: 1LU5).	21
Figure S19. 3D ligand-receptor interactions of **2b** with DNA (PDB code: 1LU5).	22

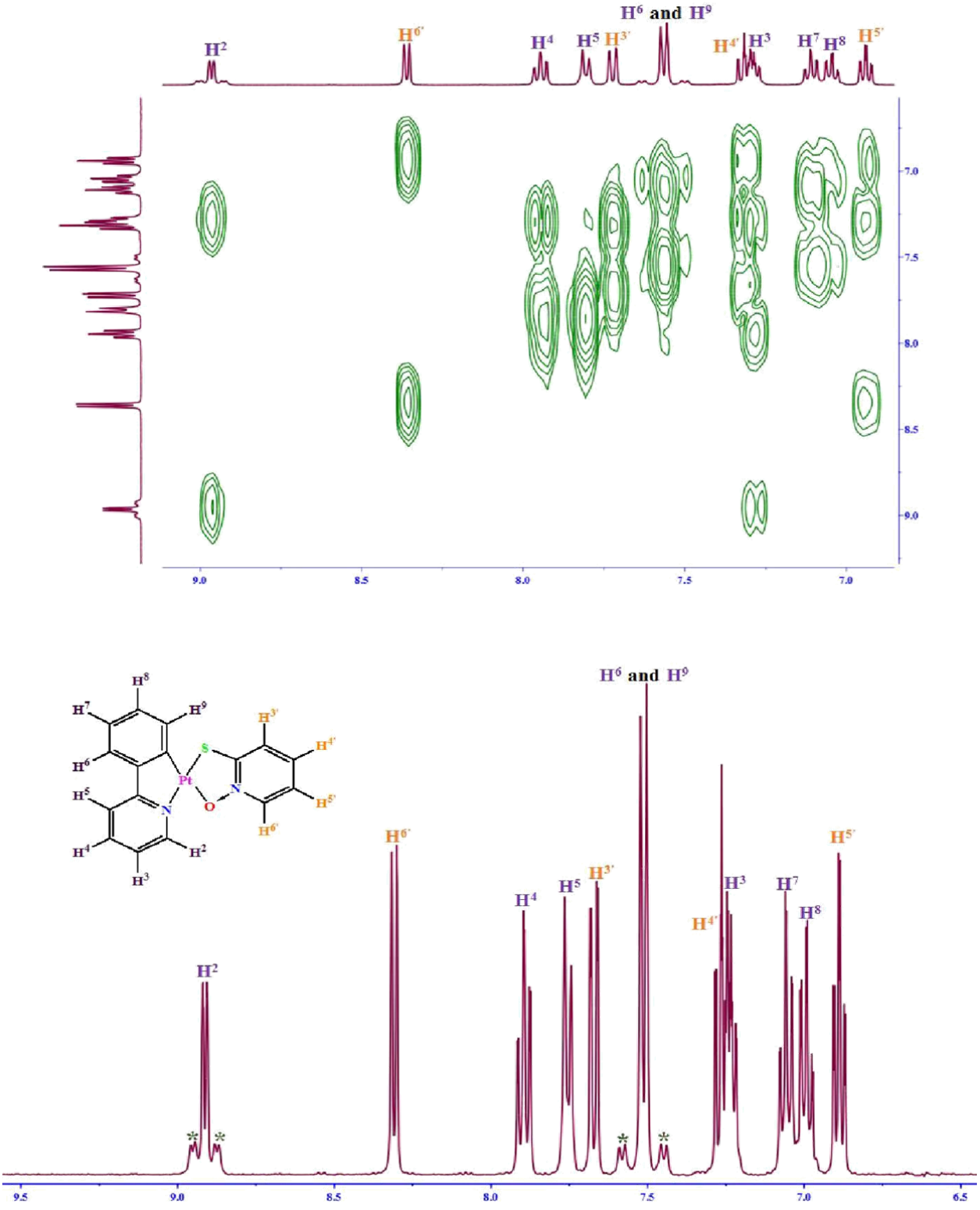

Figure S1. ^{1}H NMR (down) and HH COSY (up) spectra of **2a** in CD_2Cl_2 at room temperature. The signals assignments are depicted and the platinum satellites are indicated by *.

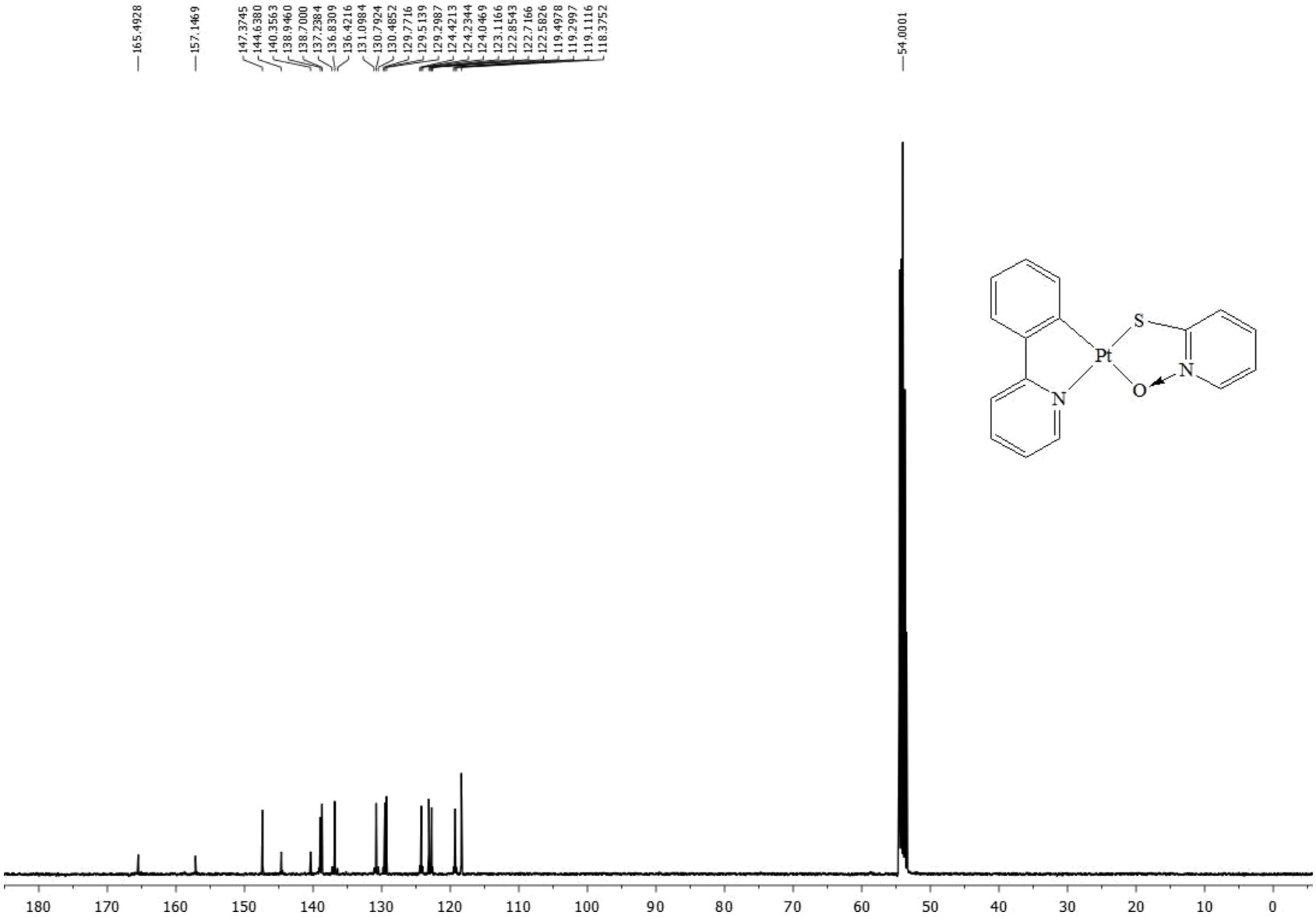

Figure S2. $^{13}C\{^{1}H\}$ NMR spectrum of **2a** in CD_2Cl_2.

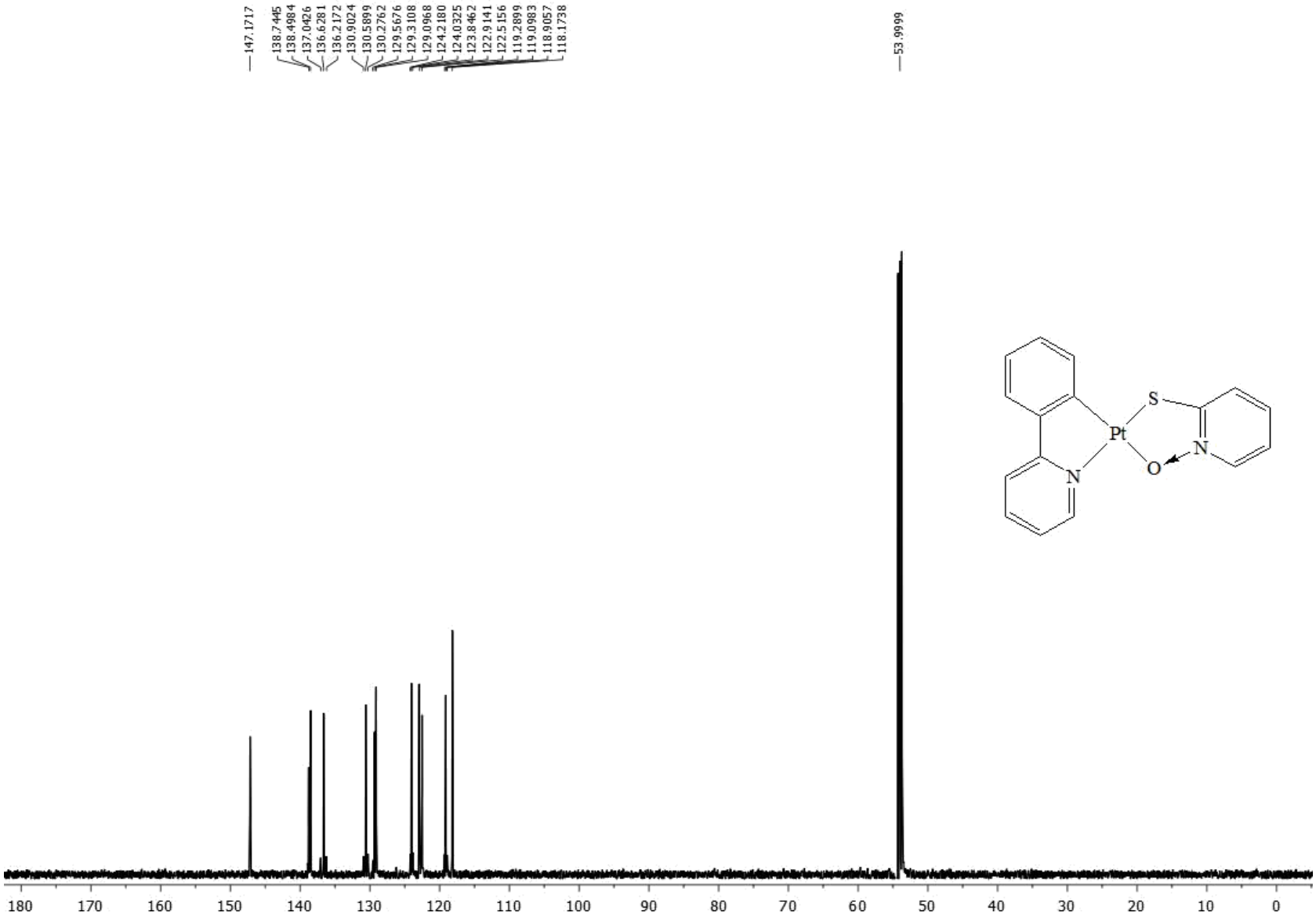

Figure S3. DEPT 135° spectrum of **2a** in CD_2Cl_2.

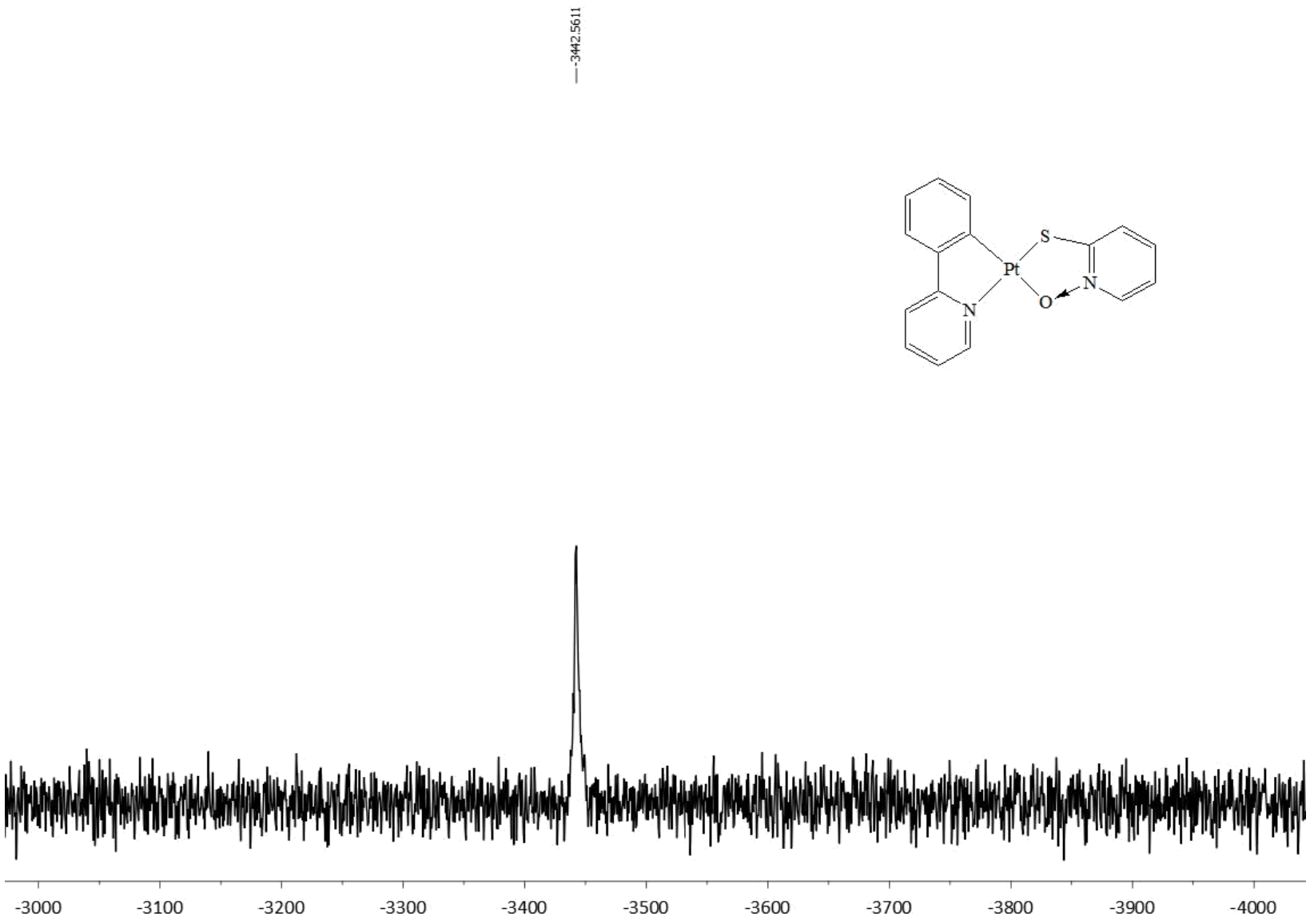

Figure S4. $^{195}Pt\{^{1}H\}$ NMR spectrum of **2a** in CD_2Cl_2.

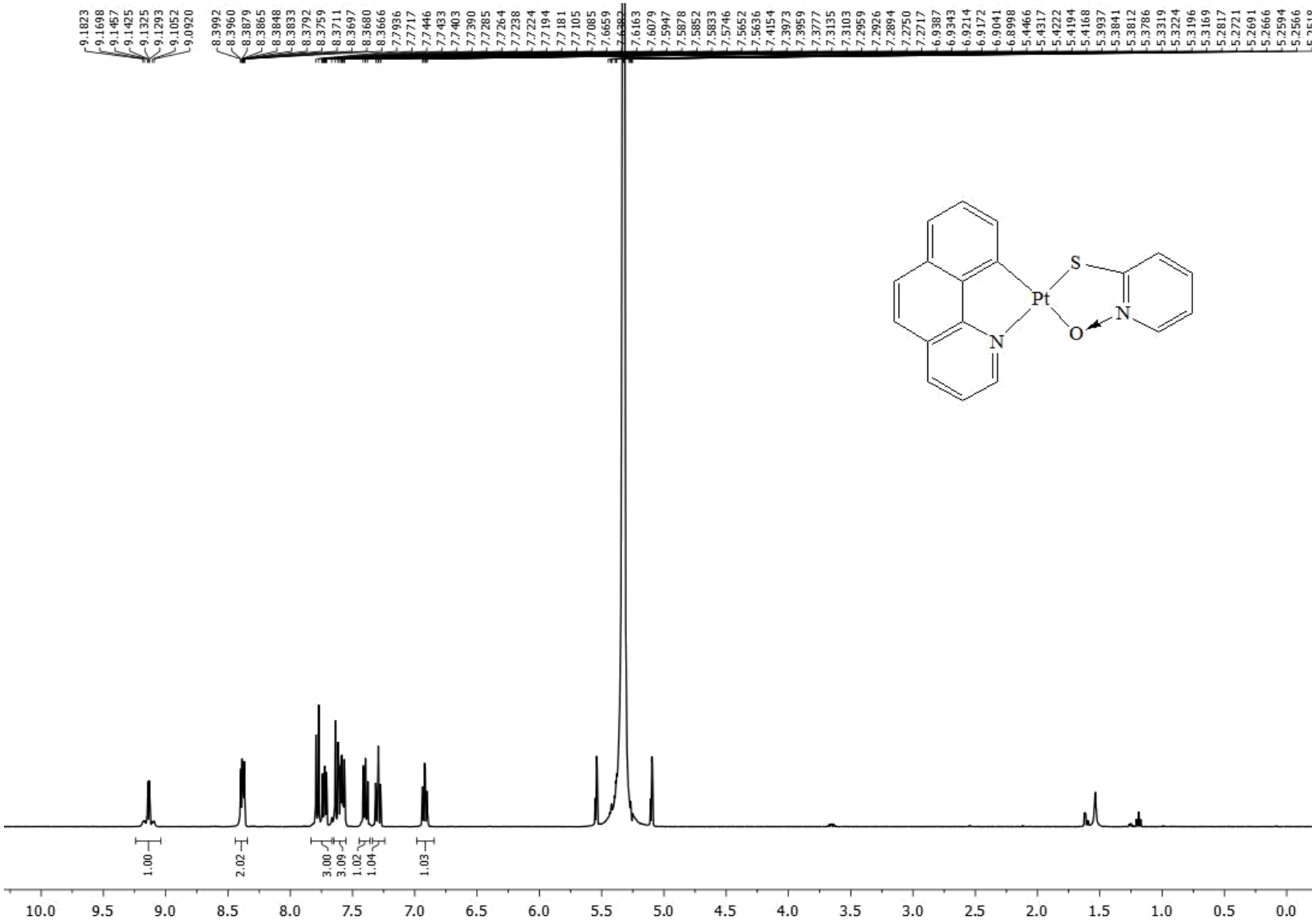

Figure S5. ^{1}H NMR spectrum of **2b** in CD_2Cl_2.

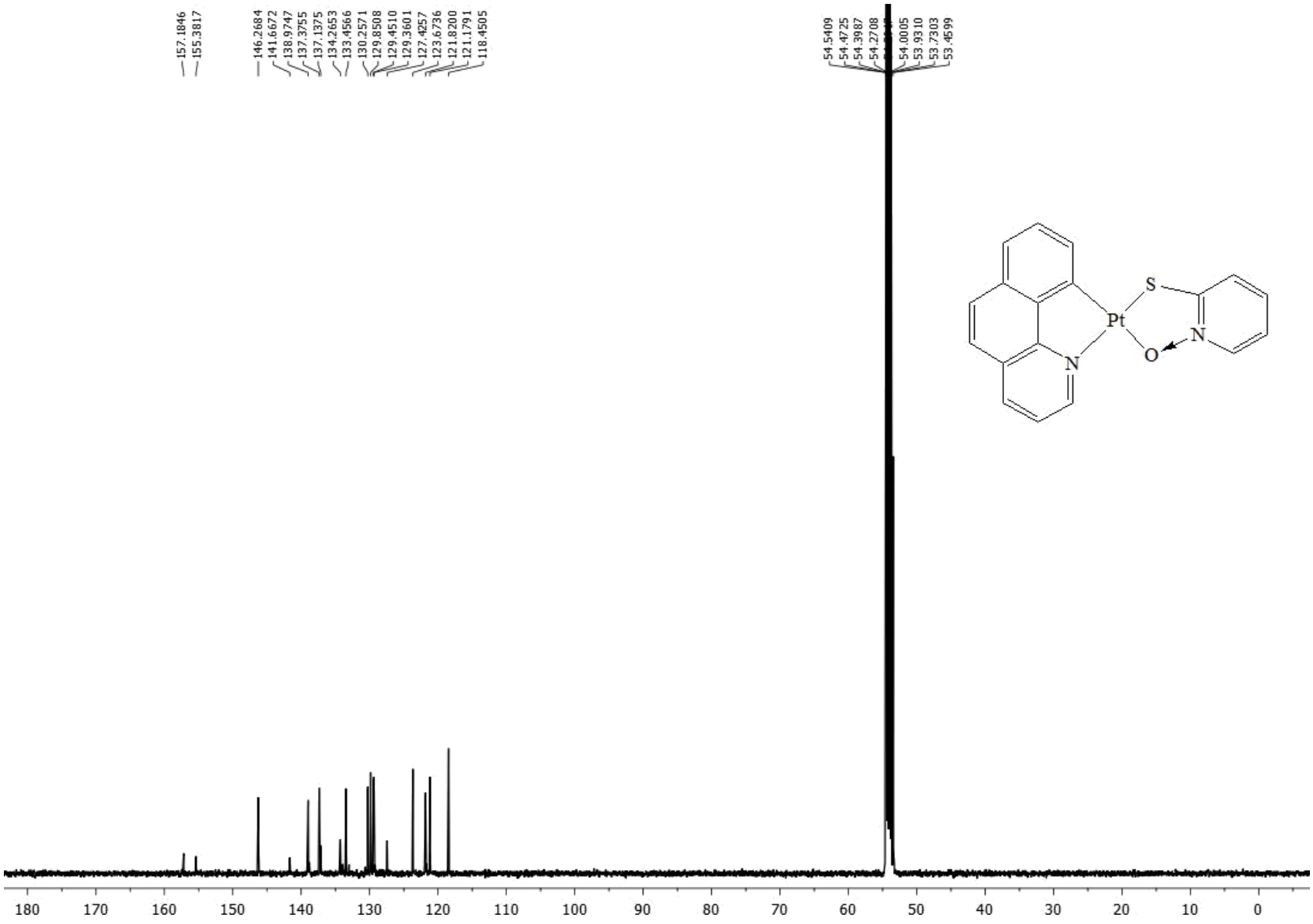

Figure S6. $^{13}C\{^{1}H\}$ NMR spectrum of **2b** in CD_2Cl_2.

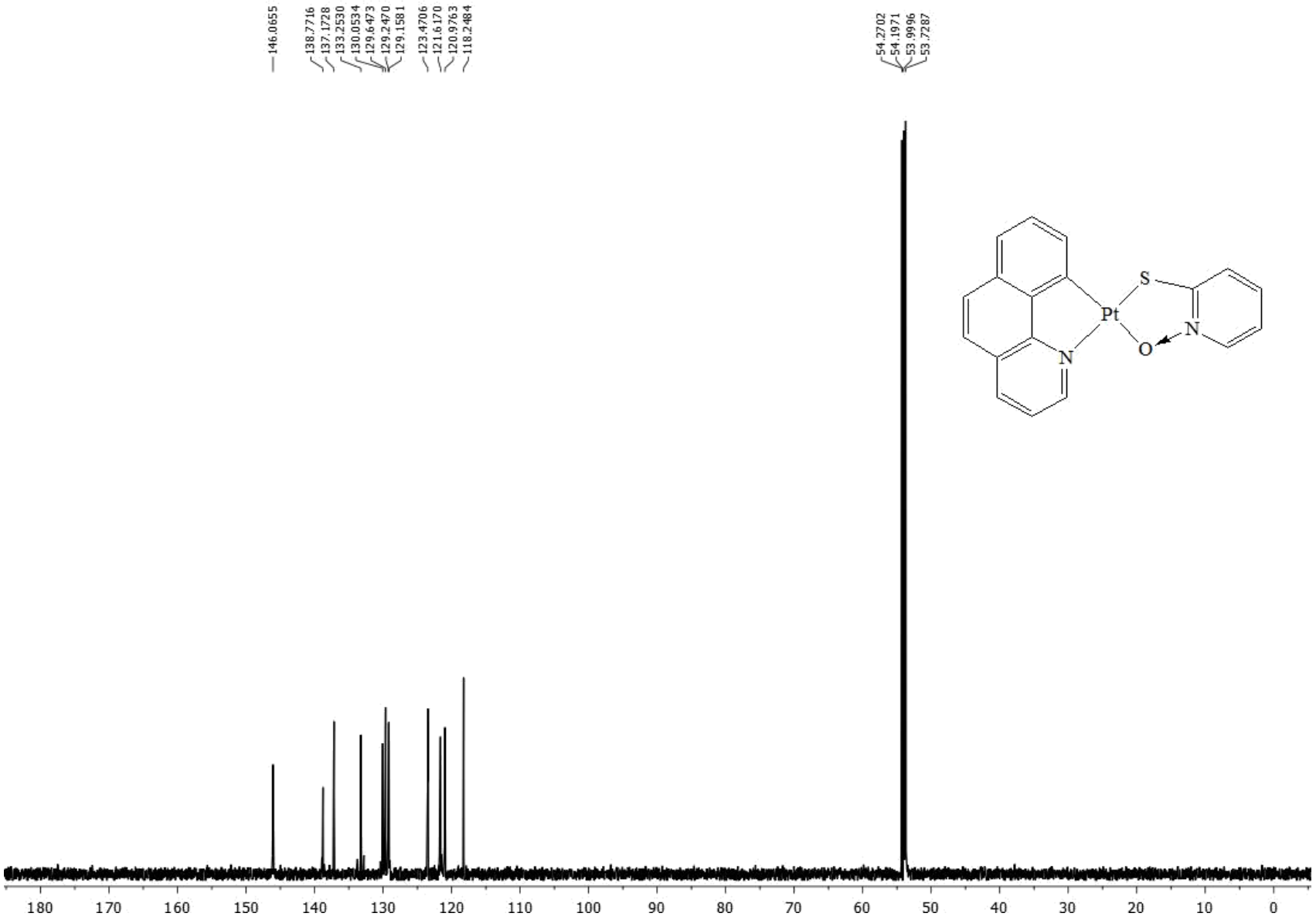

Figure S7. DEPT 135° spectrum of **2b** in CD_2Cl_2.

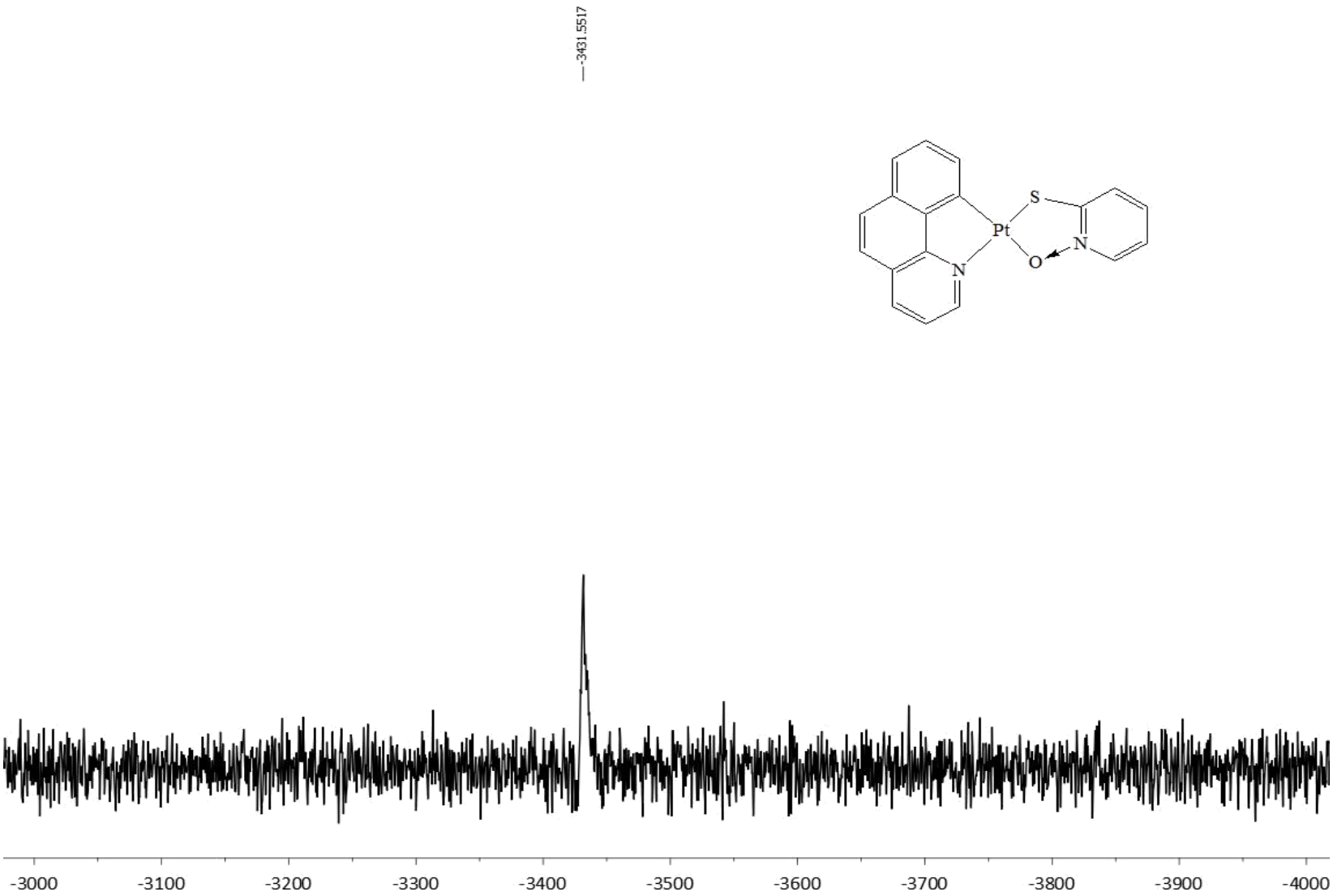

Figure S8. $^{195}Pt\{^{1}H\}$ NMR spectrum of **2b** in CD_2Cl_2.

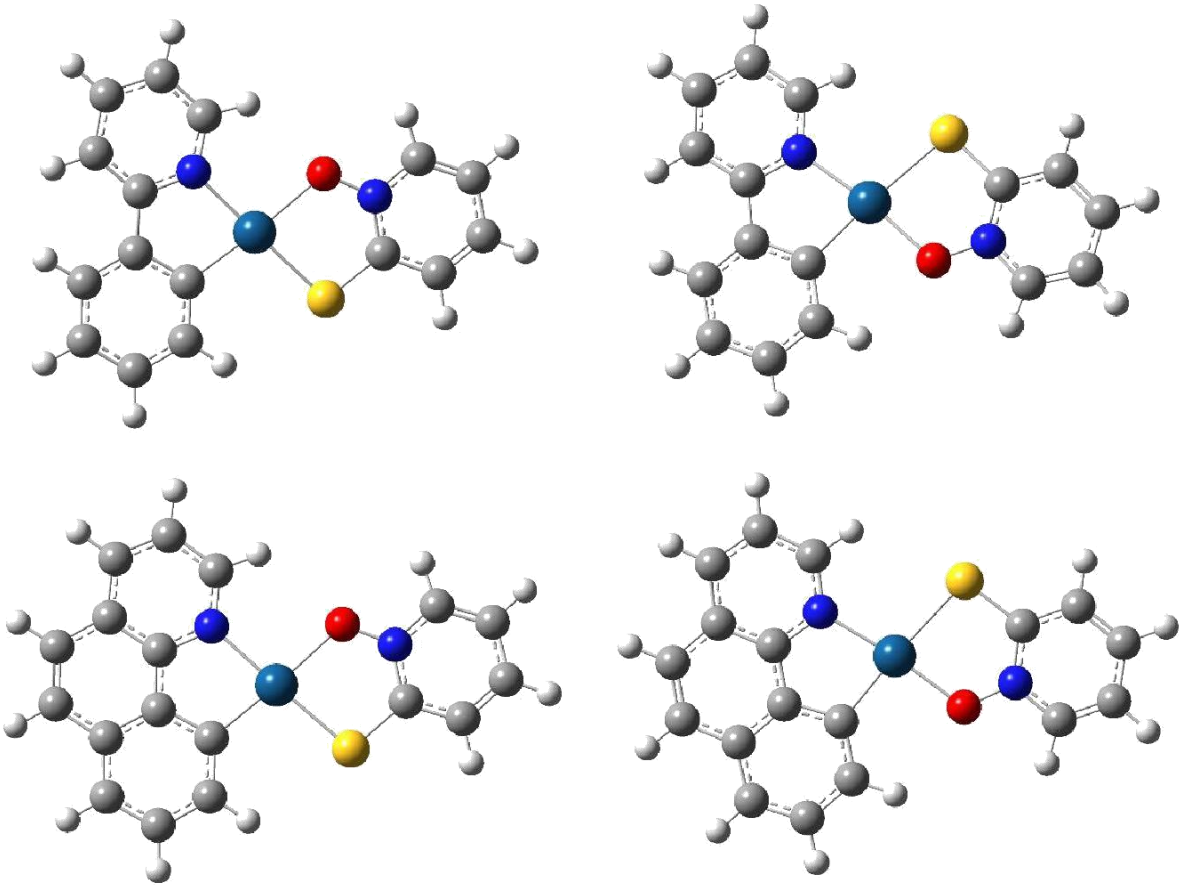

Figure S9. The calculated possible structures for SpyO ligand while it coordinated to **1**.

Table S1. Crystallographic and structure refinement data for **2a**.

Formula	$C_{16}H_{12}N_2OPtS$
Formula weight	475.42
T (K)	298(2)
λ (Å)	0.71073
Crystal system	Monoclinic
Space group	$P2_1/n$
Crystal size(mm)	0.20 × 0.10 × 0.10
a (Å)	8.6392(17)
b (Å)	8.6163(17)
c (Å)	20.066(4)
α (°)	90
β (°)	93.80(3)
γ (°)	90
V (Å^3)	1490.4(5)
Z	4
D_{calc} (g cm^{-1})	2.119
θ_{min}, θ_{max} (°)	2.57 - 25.00
F_{000}	896
μ (mm^{-1})	9.553
Index ranges	$-8 \le h \le 10$
	$-10 \le k \le 10$
	$-23 \le l \le 23$
Data collected	7906
Unique data	2624
R_1[a], wR_2[b] ($I > 2\sigma(I)$)	0.0567, 0.0728
R_1[a], wR_2[b] (all data)	0.1168, 0.0835
GOF on F^2 (S)	0.947
CCDC No.	1568889

[a] $R_1 = \Sigma||F_o|-|F_c||/\Sigma|F_o|$, [b] $wR_2 = [\Sigma(w(F_o^2-F_c^2)^2)/\Sigma w(F_o^2)^2]^{1/2}$

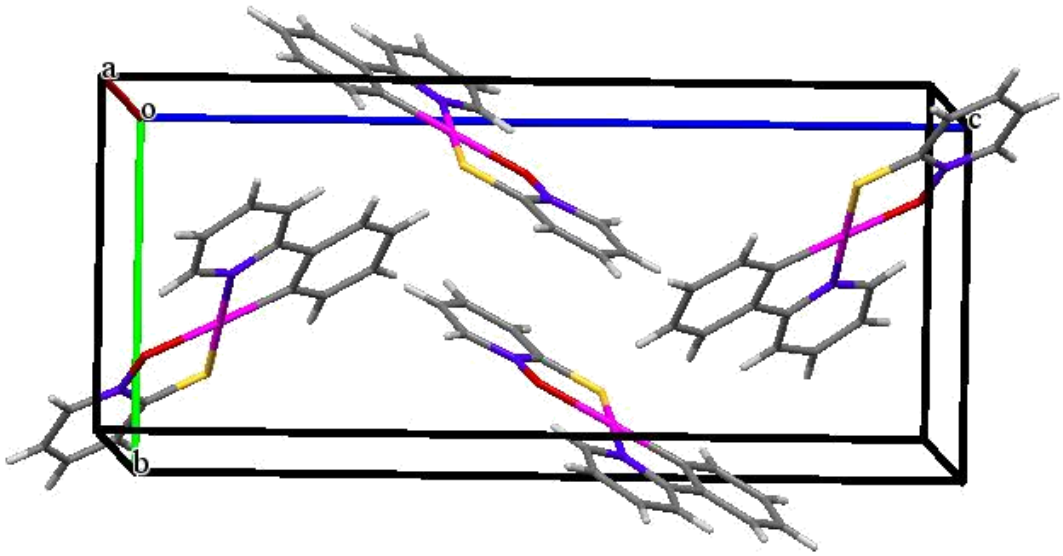

Figure S10. The crystal packing of **2a**.

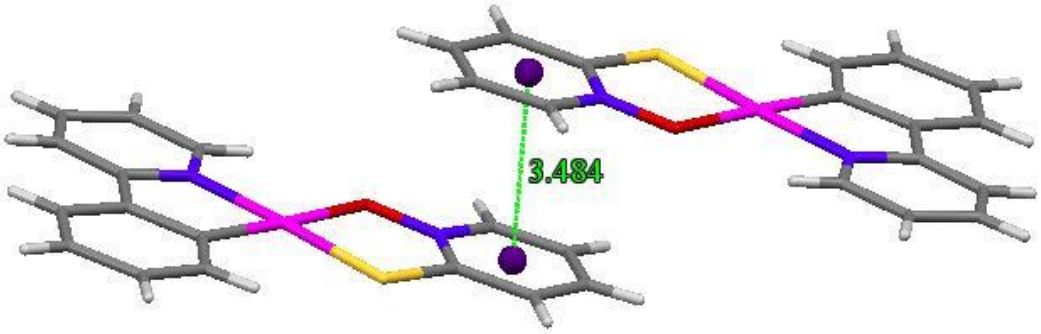

Figure S11. Complex **2a** is displaying the intermolecular contacts. The supramolecular packing is formed by dimers supported by intermolecular π···π interactions involving two SpyO ligands.

Table S2. Fragment contributions (%; from atomic orbital contributions) to the frontier orbitals of **2a** in CH_2Cl_2 solution.

Energies(eV)	Number	Pt	SpyO	ppy
-0.798	LUMO+3	1	98	1
-1.017	LUMO+2	2	2	97
-1.365	LUMO+1	1	97	2
-1.672	LUMO	6	2	91
-5.487	HOMO	36	45	19
-5.871	HOMO-1	47	28	25
-6.286	HOMO-2	94	2	3
-6.470	HOMO-3	8	8	84

Table S3. Fragment contributions (%; from atomic orbital contributions) to the frontier orbitals of **2b** in CH_2Cl_2 solution.

Energies(eV)	Number	Pt	SpyO	bzq
-0.810	LUMO+3	1	98	1
-1.216	LUMO+2	3	11	86
-1.381	LUMO+1	1	91	8
-1.844	LUMO	4	2	94
-5.433	HOMO	33	37	30
-5.784	HOMO-1	44	35	22
-6.296	HOMO-2	94	3	4
-6.425	HOMO-3	10	17	73

Table S4. Selected vertical singlet excitations of **2a** from TD-DFT calculations at the ground state geometry in CH_2Cl_2 solution (M = Pt, L = ppy, L' = SpyO).

state	Monoexcitations[a]	E/eV	λ_{cal}/nm	oscillator strength	main character
S1	H→L (63%)	3.190	389	0.114	MLCT/LC/L'LCT
S2	H-1→L (60%) H→L (31%) H→L+1 (17%)	3.364	369	0.078	MLCT/LC/L'LCT
S8	H-1→L+2 (56%) H→L+3 (22%)	4.043	307	0.067	MLCT/LC/L'LCT
S10	H→L+3 (58%) H-3→L (20%)	4.111	302	0.077	MLCT/LC/L'LCT
S14	H-1→L+3 (66%) H-2→L+4 (11%)	4.404	282	0.105	MLCT/LC/L'LCT

Table S5. Selected vertical singlet excitations of **2b** from TD-DFT calculations at the ground state geometry in CH_2Cl_2 solution (M = Pt, L = bzq, L' = SpyO).

state	Monoexcitations[a]	E/eV	λ_{cal}/nm	oscillator strength	main character
S1	H→L (66%) H-1→L (21%)	3.019	411	0.094	MLCT/LC/L'LCT
S3	H→L+1 (67%) H-1→L (16%)	3.479	356	0.065	MLCT/LC/L'LCT
S5	H→L+2 (67%) H-4→L (12%) H-1→L+1 (11%) H-1→L (10%)	3.618	343	0.146	MLCT/LC/L'LCT
S9	H-3→L (50%) H-2→L+4 (11%)	4.006	310	0.098	LC
S11	H→L+3 (56%) H-1→L+1 (24%) H-3→L (17%)	4.081	304	0.084	MLCT/LC/L'LCT
S13	H-4→L (59%) H-3→L+2 (28%) H-3→L+1 (15%)	4.181	297	0.073	LC/L'LCT

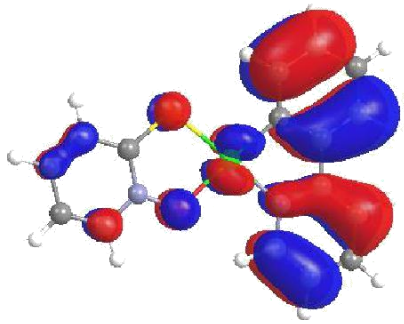

HOMO-3

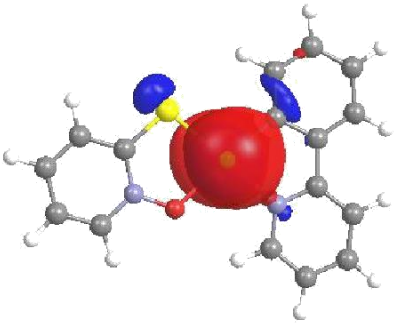

HOMO-2

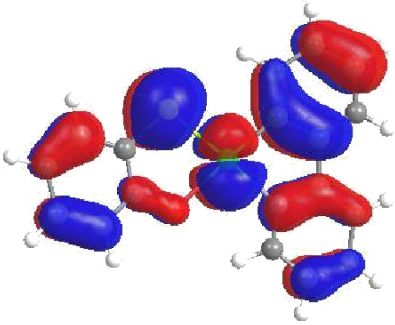

HOMO-1

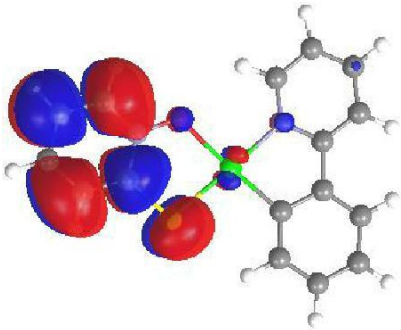

LUMO+3

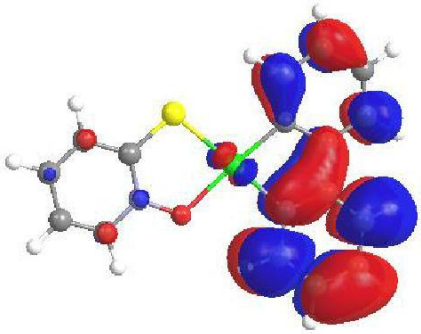

LUMO+2

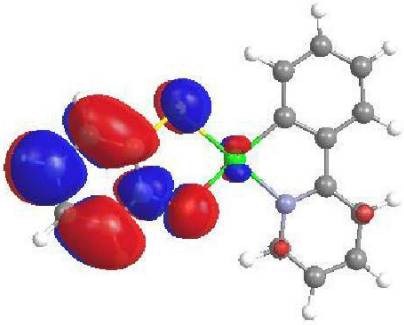

LUMO+1

Figure S12. MO plots for **2a.**

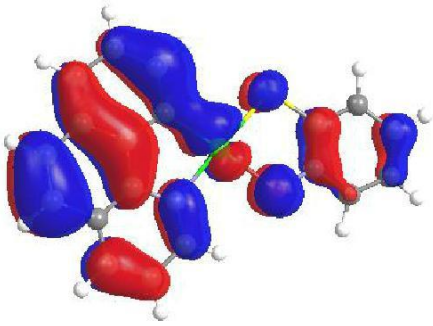

HOMO-3

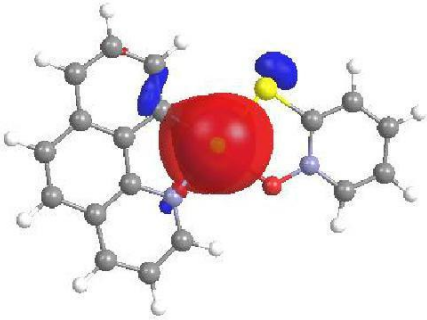

HOMO-2

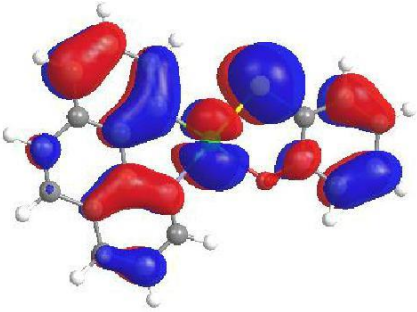

HOMO-1

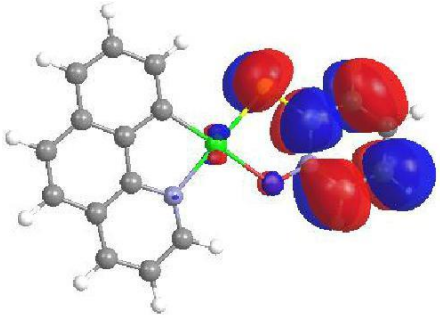

LUMO+3

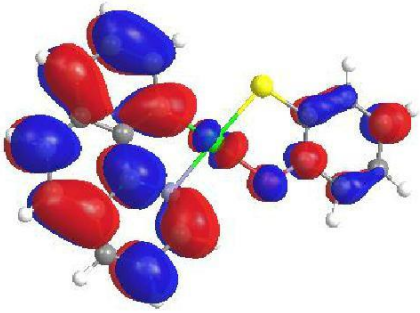

LUMO+2

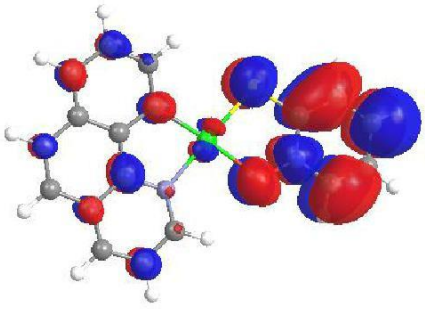

LUMO+1

Figure S13. MO plots for **2b**.

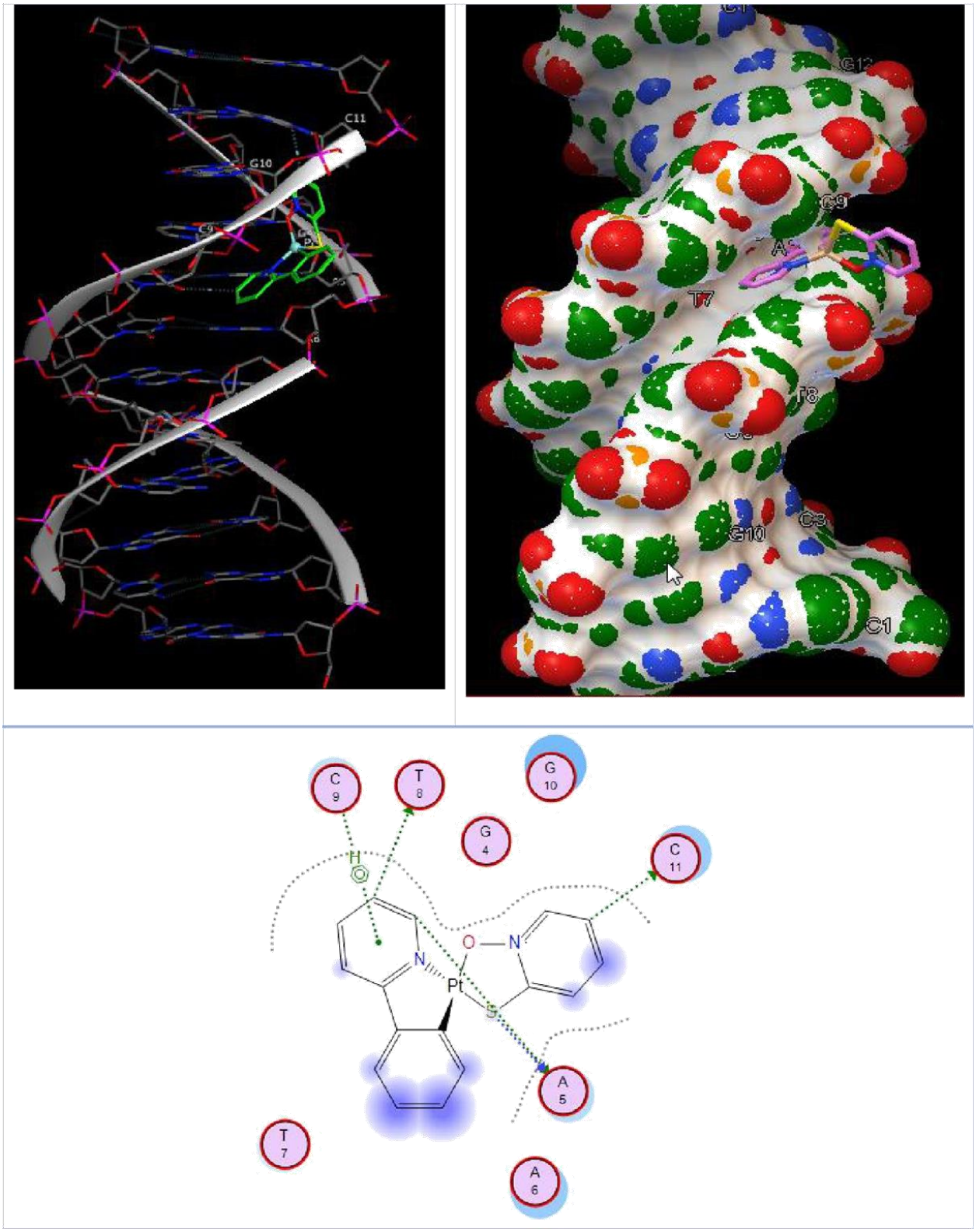

Figure S14. 3D ligand-receptor interactions of **2a** with DNA (PDB code: 1BNA).

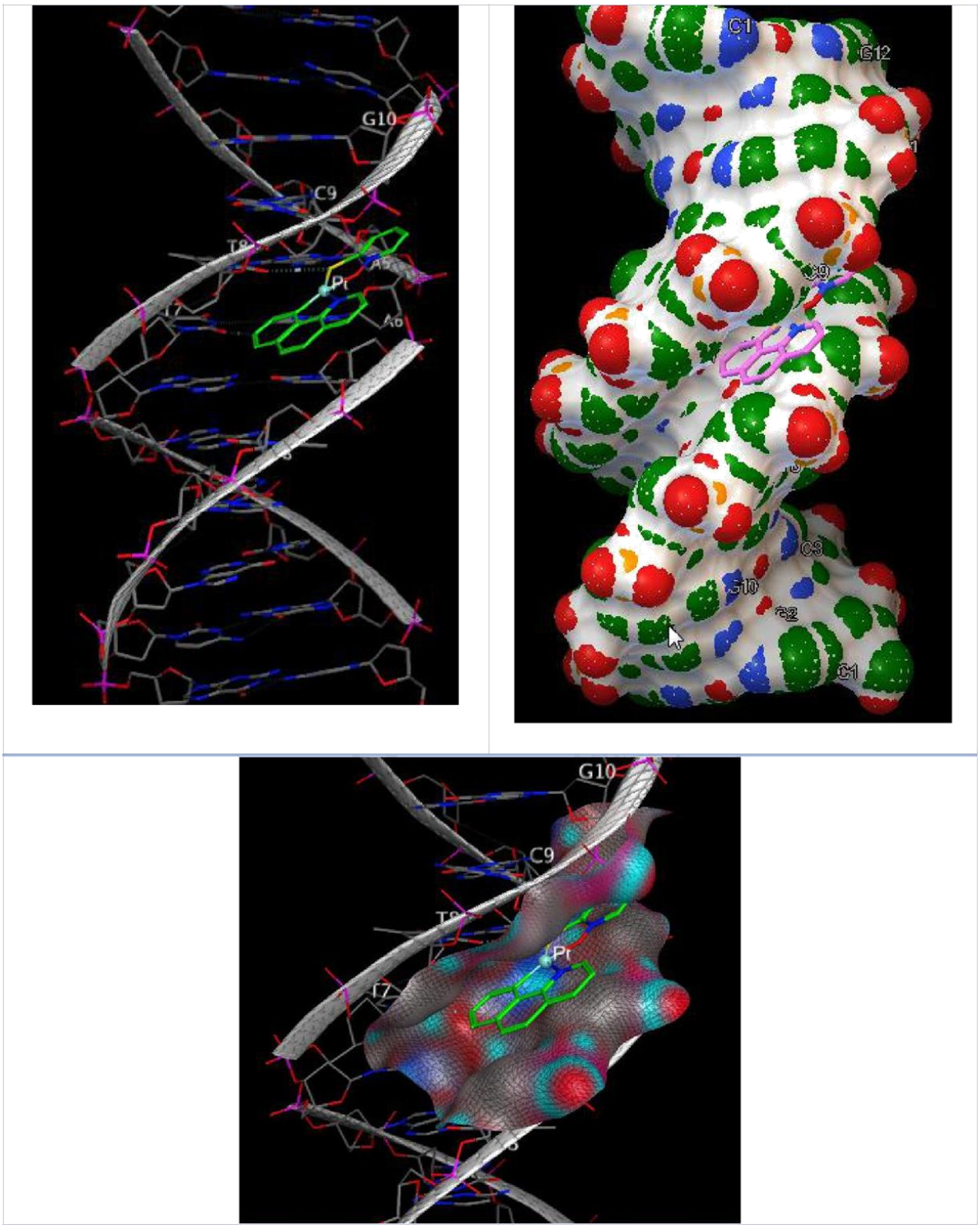

Figure S15. 3D ligand-receptor interactions of **2b** with DNA (PDB code: 1BNA).

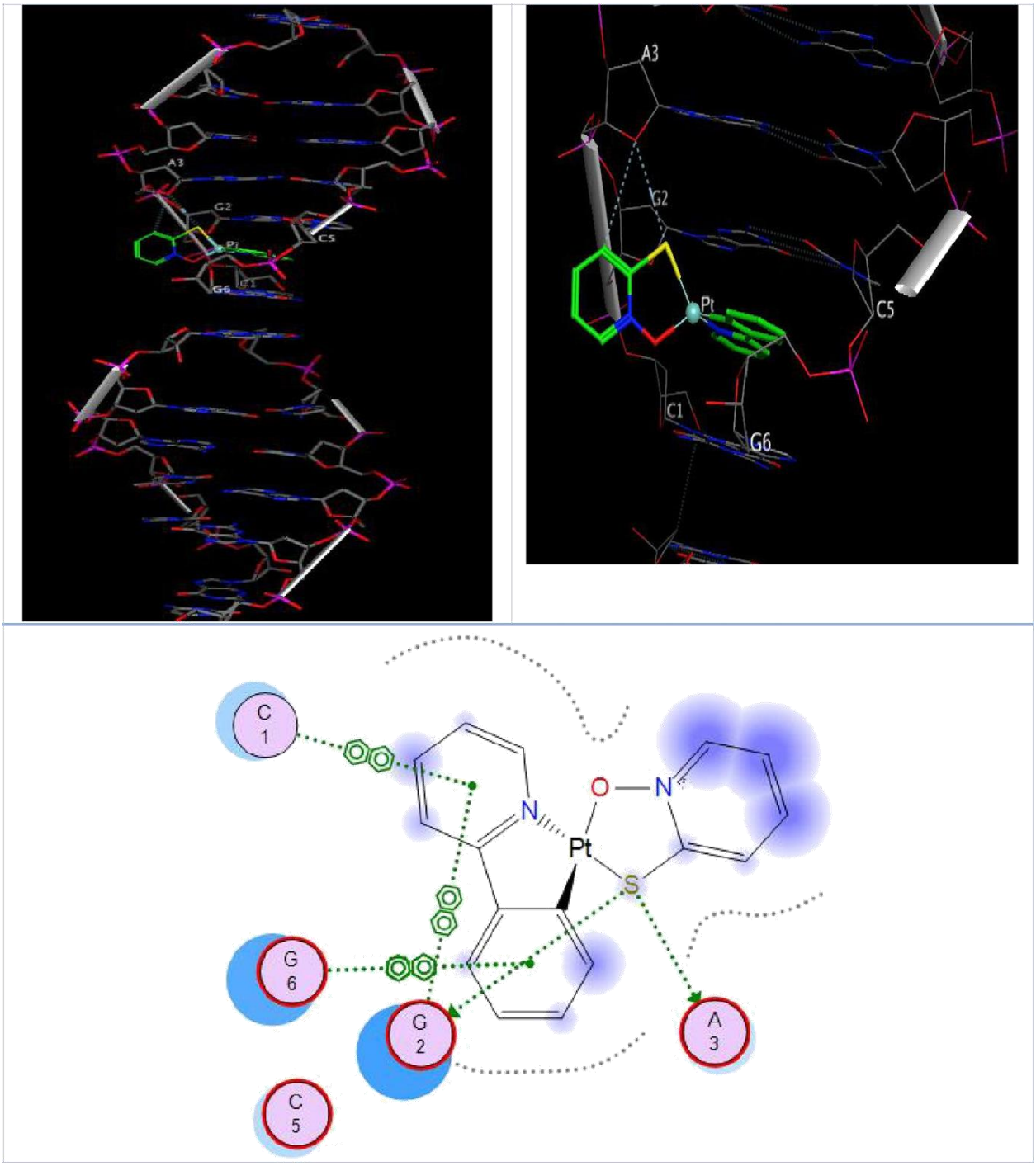

Figure S16. 3D ligand-receptor interactions of **2a** with DNA (PDB code: 198D).

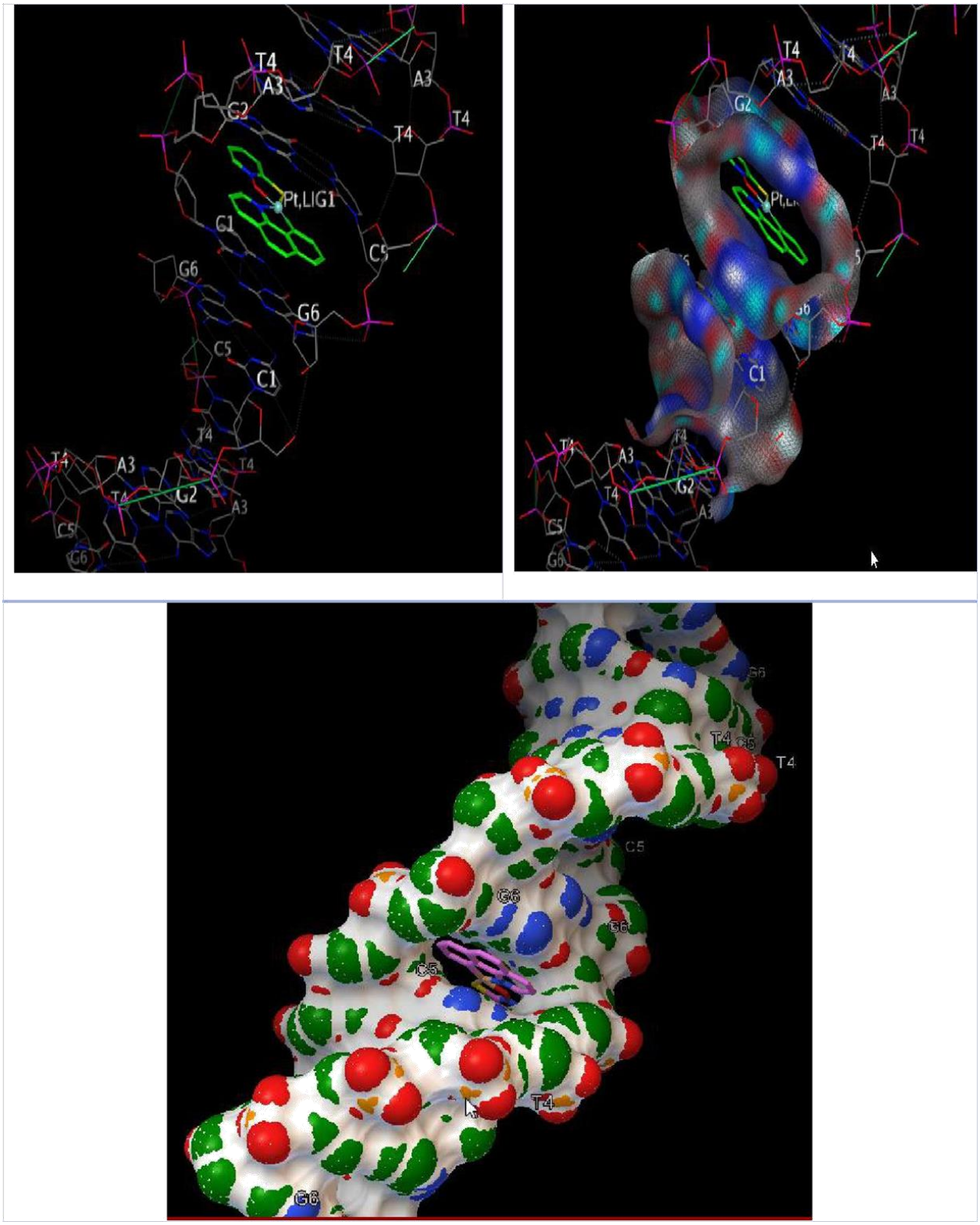

Figure S17. 3D ligand-receptor interactions of **2b** with DNA (PDB code: 198D).

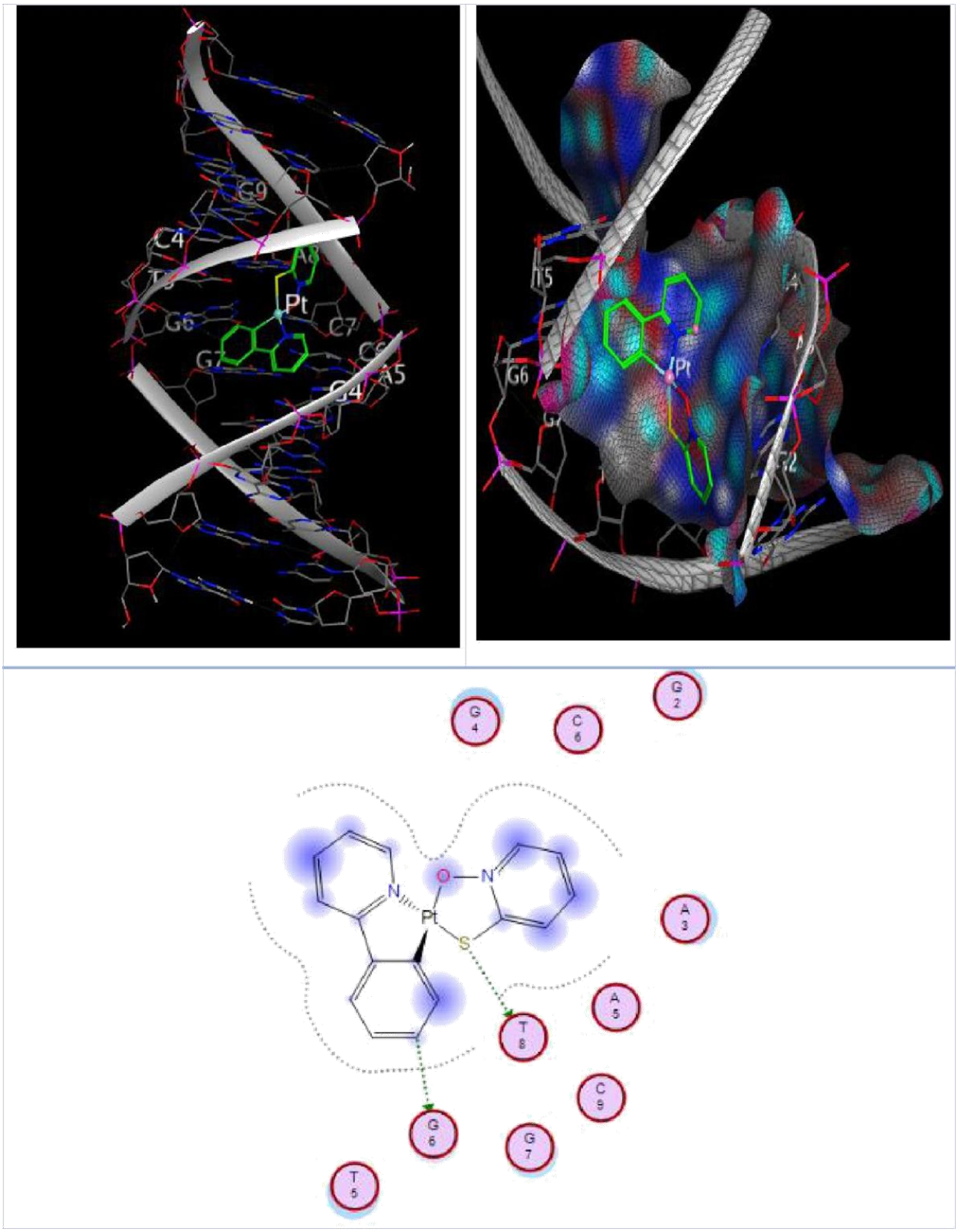

Figure S18. 3D ligand-receptor interactions of **2a** with DNA (PDB code: 1LU5).

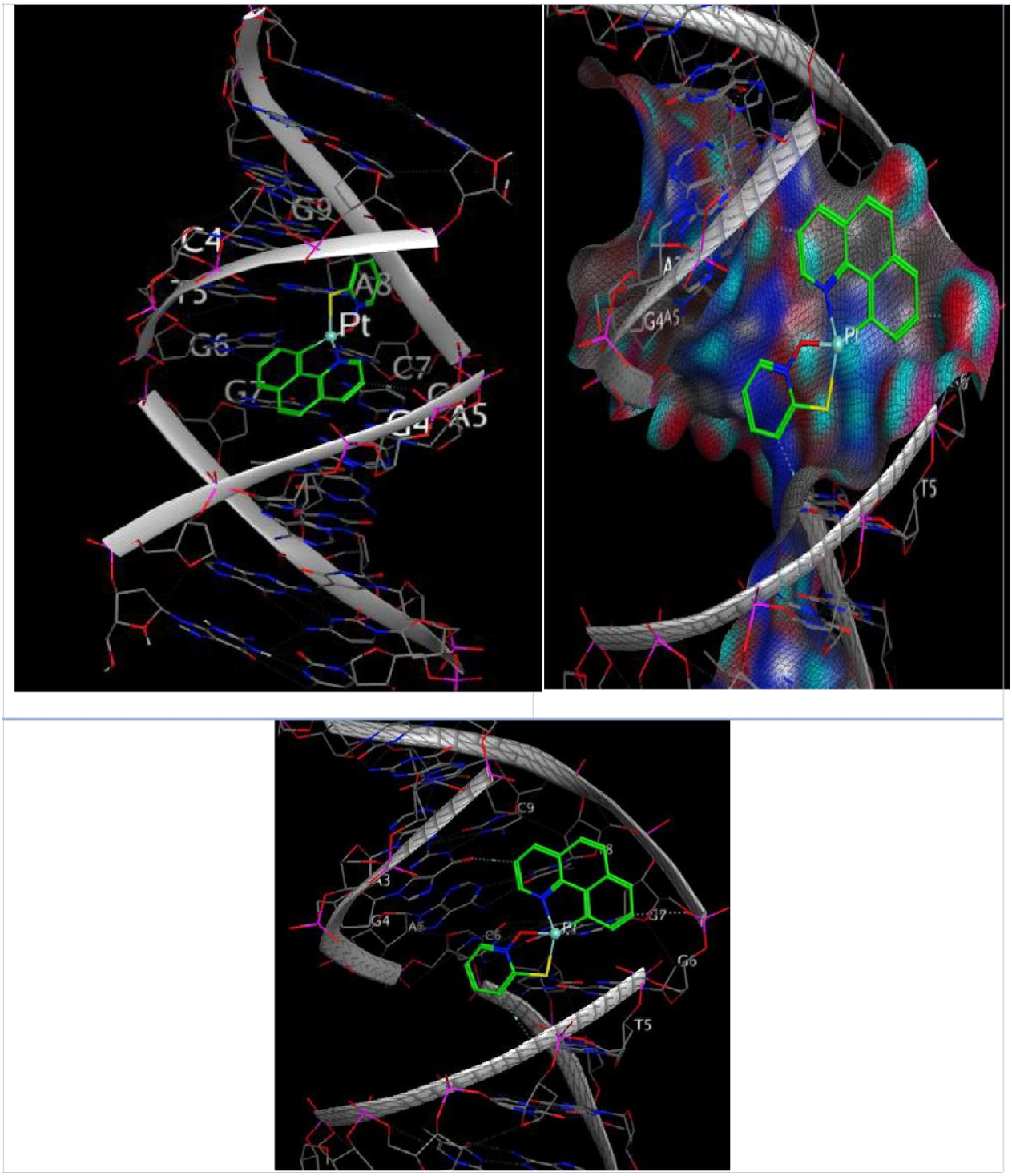

Figure S19. 3D ligand-receptor interactions of **2b** with DNA (PDB code: 1LU5).